



HAL
open science

Effect of operational parameters on the performance of a magnetic responsive biocatalytic membrane reactor

Abaynesh Yihdego Gebreyohannes, Lidietta Giorno, Ivo F.J. Vankelecom, Thierry Verbiest, Pierre Aimar

► To cite this version:

Abaynesh Yihdego Gebreyohannes, Lidietta Giorno, Ivo F.J. Vankelecom, Thierry Verbiest, Pierre Aimar. Effect of operational parameters on the performance of a magnetic responsive biocatalytic membrane reactor. *Chemical Engineering Journal*, 2017, 308, pp.853-862. 10.1016/j.cej.2016.09.057 . hal-01900377

HAL Id: hal-01900377

<https://hal.science/hal-01900377>

Submitted on 22 Oct 2018

HAL is a multi-disciplinary open access archive for the deposit and dissemination of scientific research documents, whether they are published or not. The documents may come from teaching and research institutions in France or abroad, or from public or private research centers.

L'archive ouverte pluridisciplinaire **HAL**, est destinée au dépôt et à la diffusion de documents scientifiques de niveau recherche, publiés ou non, émanant des établissements d'enseignement et de recherche français ou étrangers, des laboratoires publics ou privés.



Open Archive Toulouse Archive Ouverte (OATAO)

OATAO is an open access repository that collects the work of some Toulouse researchers and makes it freely available over the web where possible.

This is an author's version published in: <https://oatao.univ-toulouse.fr/20480>

Official URL: <http://doi.org/10.1016/j.cej.2016.09.057>

To cite this version:

Gebreyohannes, Abaynesh Yihdego and Giorno, Lidietta and Vankelecom, Ivo F.J. and Verbiest, Thierry and Aimar, Pierre Effect of operational parameters on the performance of a magnetic responsive biocatalytic membrane reactor. (2017) Chemical Engineering Journal, 308. 853-862. ISSN 1385-8947

Any correspondence concerning this service should be sent to the repository administrator:

tech-oatao@listes-diff.inp-toulouse.fr

Effect of operational parameters on the performance of a magnetic responsive biocatalytic membrane reactor

Abaynesh Yihdego Gebreyohannes^{a,b,e}, Lidiatta Giorno^c, Ivo F.J. Vankelecom^a, Thierry Verbiest^d, Pierre Aimar^{e,*}

^a Centrum voor Oppervlaktechemie en Katalyse Dept. M²S, Faculteit Bio-ingenieurswetenschappen, KU Leuven, Leuven Chem&Tech, Postbus 2461, Celestijnenlaan 200F, 3001 Leuven, Belgium

^b Department of Environmental and Chemical Engineering, University of Calabria (DIATIC-UNICAL), via P. Bucci CUBO 45^a, 87036 Rende (CS), Italy

^c Institute on Membrane Technology, National Research Council of Italy, ITM-CNR, Via P. Bucci Cubo 17C, 87036 Rende (CS), Italy

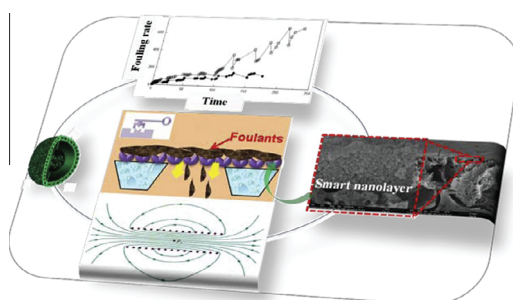
^d Molecular Imaging and Photonics, Faculty of Bioengineering Sciences, KU Leuven, Celestijnenlaan 200d - box 2425, 3001 Leuven, Belgium

^e Laboratoire de Génie Chimique, Université de Toulouse, CNRS, INPT, UPS, Toulouse, France

HIGHLIGHTS

- Magnetic stimuli-responsive biocatalytic membrane reactor was optimized.
- It was stable over a broad range of various operating parameters.
- Flux and feed concentration, related by reactor productivity were crucial parameters.
- Productivity increased with increased enzyme amount, despite the universal trend.
- There was no enzyme leakage, activity decay or TMP rise continuously over 240 h.

GRAPHICAL ABSTRACT



ABSTRACT

In this work, the performance of an innovative magnetic responsive biocatalytic membrane reactor (BMR^{SP}) has been investigated under various operational parameters. In particular, feed concentrations, flow rates across the bed, temperature and amount of biocatalytic bead were varied to probe the flow-dependent transport and kinetic properties of the reaction and the subsequent hydrolytic performance of the BMR^{SP}. The rate of fouling for the BMR^{SP} was always lower than a corresponding control system. For a given enzymatic concentration, a constant foulant hydrolyzing capacity is identified. At 3 g/m² pectinase containing bionanocomposites, the BMR^{SP} hydrolytic efficiency was 1.5 g/m² h. This efficiency was further increased by increasing the amount of bionanocomposites per membrane area. This further allowed the BMR^{SP} to hydrolyze higher loads of foulants while keeping a low if not zero increase in TMP over time at constant flux.

Identification of an optimal operating condition laid the platform for continuous operation of the BMR^{SP} over 200 h, without visible transmembrane pressure drift while maintaining constant flux. Product assay in the permeate gave constant value in the entire duration, i.e., no enzymatic activity decay owing to

Keywords:

Biocatalysis
Membrane fouling
Nanocomposite
Magnetic nanoparticle
Packed bed reactor
Stimuli-responsive membrane

Abbreviations: Enz^{SP}, enzyme functionalized superparamagnetic nanoparticles; M^{SP}, superparamagnetic membrane; TMP, transmembrane pressure; BMR^{SP}, superparamagnetic biocatalytic membrane reactor; NP^{SP}, superparamagnetic nanoparticles; DMF, dimethylformamide; PVDF, polyvinylidene fluoride; GalA, galacturonic acid; APTMS, 3-aminopropyl trimethoxysilane; PEG, polyethylene glycol; BCA, bicinchoninic Acid; Pe, Peclet number; J_{opt}, optimum flux (L/m² h); SEM, scanning electron microscopy.

* Corresponding author.

E-mail addresses: abayneshy@yahoo.com (A.Y. Gebreyohannes), l.giorno@itm.cnr.it (L. Giorno), ivo.vankelecom@biw.kuleuven.be (I.F.J. Vankelecom), thierry.verbiest@fys.kuleuven.be (T. Verbiest), Pierre.Aimar@univ-toulouse.fr (P. Aimar).

stable enzyme immobilization and no leakage through the pores of the membrane owing to the synergistic magnetic interaction between the magnetic membrane and magnetic bionanocomposites.

The obtained stability over a broad range of operational parameters and sustainable performance over long period gives a high prospect to the newly developed BMR^{SP} to be utilized in continuous biocatalysis and separation, thereby significantly improved process efficiency.

1. Introduction

An immobilized enzyme membrane reactor provides the platform for a continuous reactor operation without the need for an additional step to recover the enzyme [1–3]. The average residence time within the reactor is far shorter for the substrate than for the immobilized enzyme, resulting in a high productivity compared to a batch operation in similar conditions [4].

Immobilized enzymes cannot however be replaced with fresh enzyme neither can the membrane be easily cleaned when the whole structure gets oversaturated with substrate or the enzyme is deactivated.

To surmount these major challenges, the concept of a magnetic stimuli-responsive biocatalytic membrane reactor has been investigated, that can reversibly immobilize enzymes on a membrane by effectively switching on or off an external magnetic field [5].

The system contains enzyme functionalized superparamagnetic nanoparticles (bionanocomposites; Enz^{SP}) and a “smart” paramagnetic polymeric membrane (M^{SP}). The application of an external magnetic field parallel to the surface of the M^{SP} induces the Enz^{SP} which are initially dispersed in the bulk stream to align along the applied magnetic field and to be attracted towards the M^{SP} to form a biocatalytic layer [6–8]. The voids between the Enz^{SP}s connected head-to-tail by magnetic forces form as many micro-reactors. The system applied to the in-situ degradation of pectins and arabinoxylans showed an interesting performance. Moreover, thanks to its magnetic responsiveness and absence of residual magnetic memory in the absence of an external magnetic field, it was possible to easily recover the Enz^{SP} and use both the enzyme and membrane over many cycles.

The accumulation of particles or solutes rejected by the so formed composite membrane can however lead to less flux at fixed transmembrane pressure (TMP) or a higher TMP for a given constant flux [9]. This eventually would result in a short operational period, frequent cleaning and premature replacement of the biocatalyst.

An increase in mass transfer resistance or an enzyme activity loss have a similar effect on the biocatalytic membrane reactor performance. The mechanisms to control them however are very different [10] and require a fine control of process parameters such as feed flowrate, feed and enzyme concentration and reaction temperature [11].

Thus, the main objective of this paper is the detailed investigation of the effect of different operational parameters on the efficiency and stability of the BMR^{SP}. The different operational parameters considered include: flux to control the mass transfer rate, temperature, feed concentration and enzyme concentration to control the reaction rate. The design of a continuous flow immobilized enzyme membrane reactor requires the knowledge of the enzyme kinetic parameters which have been assessed for the Enz^{SP} in a flow-through continuous flow biocatalytic membrane reactor.

1.1. Background

Due to simultaneous reaction and separations, absence of enzyme-product inhibition can be assumed [1–3]. Therefore, the

initial reaction rate (v_r) in a continuous flow reactor can be calculated based on the following mass balance equation [4,12]:

$$\frac{d(VC)}{dt} = (FC)_{in} - (FC)_{out} + v_r V_a \quad (1)$$

where F is the feed flowrate (L/s), C is the concentration (g/L), v_r is the volumetric reaction rate (g/L s) and V_a is the reactor volume (L). At steady state the accumulation term is zero and the reaction rate is:

$$v_r = \frac{F(C_f - C_p)}{V_a} \quad (2)$$

where C_f and C_p are substrate concentration in the feed and in the permeate (g/L) respectively. The BMR^{SP} is made of bed of catalytic beads supported by a flat sheet membrane. The actual reactor volume (V_a) is the void volume, i.e. the fraction of the bed volume that is not filled with catalyst:

$$V_a = V_T - V_p \quad (3)$$

where V_p is the volume of the Enz^{SP} beads present on the surface of the membrane and V_T is the total bed volume (dm³) given by the BMR^{SP}'s geometric dimensions as:

$$V_T = L * A_m \quad (4)$$

where L is the catalytic bed thickness in dm (e.g. obtained from SEM micrographs in Fig. 2), while A_m is the membrane area (0.16 dm² in the present work).

V_p can be calculated as:

$$V_p = \frac{m_p}{\rho_p} \quad (5)$$

where m_p is the total mass of Enz^{SP} (4.8 * 10⁻³ g) deposited on the membrane and ρ_p is the density of ferrous particles (5150 g/L).

By combining Eqs. (3)–(5), the volume of the reactor is then:

$$V_a = LA_m - \frac{m_p}{\rho_p} \quad (6)$$

By combining Eqs. (2) and (6), the following equation is obtained for the volumetric reaction rate, v_r (mol/L h):

$$v_r = \left\{ \frac{F\rho_p}{L\rho_p A_m - m_p} * (C_f - C_p) \right\} / M_{wt} \quad (7)$$

where M_{wt} is the molecular weight of the hydrolysis product.

2. Materials and methods

2.1. Materials

Dimethylformamide (DMF) was acquired from Arcos. Polyvinylidene fluoride (PVDF, 534 kDa), 2-cyanoacetamide, citrus fruit pectin (25–35% degree of esterification), polygalacturonase, galacturonic acid (GalA; M_{wt} : 212 g/mol) and glycine were obtained from Sigma-Aldrich (France). Borate buffer solution (pH 9.2) was supplied by Fisher scientific and methoxy(polyethyle

neoxy)-propyltrimethoxysilane(PEGSilane),(3-aminopropyl)trimethoxysilane (APTMS) by ABCR chemicals.

2.2. Methods

2.2.1. NP^{SP} synthesis

The NP^{SP} used as nanofillers during membrane preparation were iron oxide nanoparticles with an average particle size of 8 nm [5] coated with polyethylene glycol (PEG). Analytical grade ferric trichloride (FeCl₃) was used as salt precursor, ethylene glycol as both solvent and reductant, and n-octylamine as capping agent. Typically, 37.5 mL ethylene glycol and 25 mL n-octylamine were transferred into a flask and heated to 150 °C. In a beaker, 2.4 g FeCl₃ was dissolved in 10 mL ethylene glycol and 3.5 mL purified water. After dissolving the salt, the ferric chloride solution was slowly added to the flask and further heated to reflux at 180 °C for 24 h. The thermal decomposition of the FeCl₃ is frequently carried out in hot solvent containing surfactants e.g., n-octylamine, to control particles growth and prevent particle agglomeration [13,14]. A highly polar solvent, ethylene glycol, was chosen since it can simultaneously serve as solvent and reducing agent, while it also provided enough hydrophilicity [13].

The n-octylamine coated nanoparticles (100 mg) were then silanized by mixing with 1 mL PEG-Silane (9–12 PE units) together with trace amounts of acetic acid to form dried PEG coated nanoparticles that can easily be re-dispersed in a desired solvent (e.g. water or DMF). The acetic acid acted as a catalyst for the hydrolysis and the condensation of silane groups on the particles surface and thus for the surface exchange reaction as a whole. The PEG silanized NP^{SP} dispersed in DMF were then used as nanofillers during membrane preparation.

2.2.2. Enzyme immobilization on aminated NP^{SP} to form Enz^{SP}

To enable the coupling of enzymes to the surfaces of NP^{SP}, APTMS was used as a coating layer instead of PEG so as to introduce reactive amine groups on the surface of the NP^{SP}. This was achieved by reaction of 100 mg n-octylamine coated iron oxide nanoparticles dispersed in 100 mL methanol with 1 mL APTMS (179 g/mol) and 3 drops of acetic acid under sonication. A detailed description of the preparation and characterization of both the PEG coated and the aminated NP^{SP} is given elsewhere [15].

All enzyme immobilizations were performed using glutaraldehyde as a crosslinker. 2.4 mg of aminated NP^{SP} in sodium acetate buffer (100 mM; pH 4.5) were washed three times with deionized water before mixing with 0.8 mL of a 25% aqueous glutaraldehyde solution and stirred for 2 h at room temperature to introduce a terminal aldehyde functional group on the NP^{SP}. Non-reacted glutaraldehyde was removed by washing the particles with distilled water.

The aldehyde derivatized NP^{SP} were then mixed with 1.2 mL of a solution of 20 g/L of polygalacturonase (EC232-885-6). The pectinase was dissolved in sodium acetate buffer (pH 4.5, optimal for pectinase). Out of preliminary experiments, an immobilization time of 10 h was found to keep the immobilized activity at its maximum level. The reaction mixture was left on a shaker at 150 rpm and room temperature to form the biocatalytic superparamagnetic nanoparticles with immobilized pectinase (Enz^{SP}). Shaking was necessary to keep the particles suspended in the reaction mixture [5]. In order to block the excess of activated aldehyde group on the Enz^{SP}, the reaction was quenched with (1 mL; 1 M) of glycine [16].

2.2.3. Membrane preparation and characterization

To prepare the M^{SP}, dope solutions containing 12% PVDF in DMF were prepared with variable PEG coated NP^{SP} concentrations (0.08–0.5 w/w%). Before casting, the dope solution was mixed using a custom-made mechanical rotator and sonicated to disperse

the NP^{SP} in the dissolved polymer. Further details can be found in our previous work [5]. The M^{SP} prepared from 0.33 w/w% NP^{SP} (highest flux and lowest fouling propensity: results found from preliminary characterization) were selected for the BMR^{SP} application in this work.

2.2.4. Membrane pore size, pore size distribution and SEM analysis

For the membrane containing, 0.33 wt% NP^{SP}, pore size and pore size distribution was compared in the presence and absence of a dynamic layer of Enz^{SP}. The measurement was done on a 1500-AEHL capillary flow porometer (Porous Media Inc., Ithaca, NY). 'Pore wick' with a defined surface tension of 16 dynes/cm (Porous Media Inc., Ithaca, NY) was used as the wetting liquid. The dynamic layer on the surface of the membrane was formed by depositing 3 g/m² Enz^{SP}. The membrane was then oven dried at 60 °C for 2 h before the measurement.

The microstructure of the M^{SP} was also observed by scanning electron microscopy (SEM, Philips SEM XL30 FEG with Adax dx-4i system).

2.2.5. Reaction conditions

A reaction of Enz^{SP} with model pectin solution was carried out at 40 ± 3 °C in convective flow mode (continuous flow). The membrane with an area of 0.0016 m² was mounted in a 50 mL Amicon™ filtration cell. The feed solution was supplied continuously using a syringe pump at constant flowrate (PHD 2000 Syringe, Harvard instruments). The separation characteristics of the selected membrane allow the total rejection of pectin and zero rejection of the hydrolysis product, GalA. It is worth noting that a complete removal of GalA from the BMR^{SP} is crucial since it has an inhibitory effect on the pectinase [17]. The degree of conversion in the BMR^{SP} was calculated as the ratio of the molar concentrations of GalA in the permeate to the pectin concentration in the feed. The bench scale reactor was immersed in a water bath for temperature control. The TMP was monitored using LEO 2 micro-processor controlled pressure gauges. A circular permanent magnet with a diameter of 5 cm was located underneath the filtration cell (Fig. 1). The permeate flow rate through the membrane was varied from 5 to 70 mL/min. The range of parameters that were varied during the experiment are: feed concentration (0.01–0.3 g/L), flux (5–45 L/m² h), temperature (25–40 °C) and Enz^{SP} loading (1–9 g NP^{SP}/m² membrane area) corresponding to 0.24 to 2.16 g/m² of immobilized enzyme. Samples (1 mL) were collected at different times for product assay from the permeate line and stored at –20 °C until further analysis.

The produced galacturonic acid (GalA) was determined according to the 2-cyanoacetamide method [18]. The method is based on a Knoevenagel condensation reaction between an active methylene group of cyanoacetamide and the aldehyde group of GalA to form an ultraviolet absorbing product [19]. A 2-cyanoacetamide (1%, 1 mL) was added to 1 mL of hydrolysate that was collected from the permeate line of the BMR^{SP}. This was then mixed with 2 mL of 100 mM cold borate buffer at pH 9 and vortex mixed. Subsequently, the mixture was heated to 100 °C for 10 min. After cooling down to room temperature, the absorbance at 274 nm was measured on a Shimadzu 1650PC spectrophotometer against distilled water. The concentration of GalA was calculated from the standard curve obtained by using solutions of GalA dissolved in the buffer at different concentrations (0.1–2 μM). In addition to enzymatic hydrolysis, GalA can also form when a pectin solution is heated due to β-hydrolysis, although the rate of reaction is slow at pH 4.5 [20]. In order to account for this, a known volume of pectin solution was heated at 40 °C and 100 °C. These values were then taken as background to calculate the actual release of GalA due to enzymatic hydrolysis.

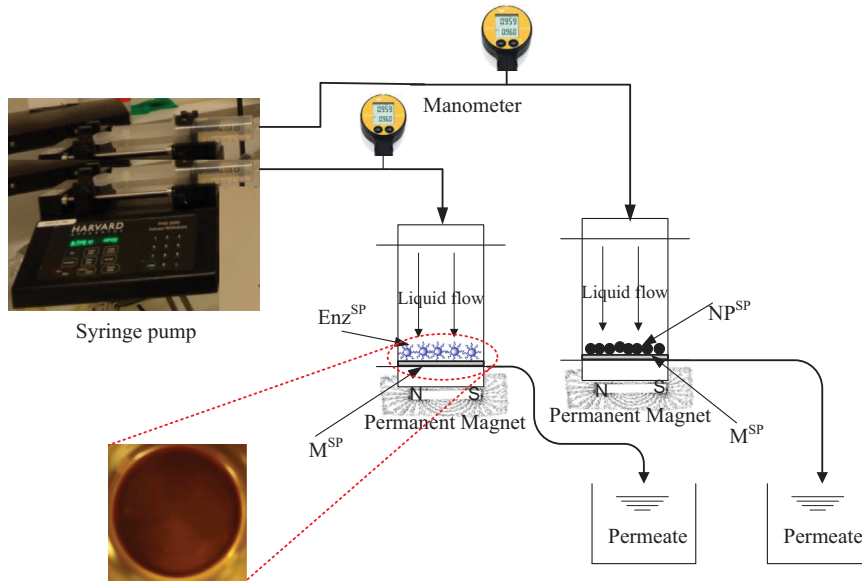


Fig. 1. Schematic illustration of the filtration set-up containing a syringe pump with two heads, two syringes each with 100 mL capacities, dead end filtration cell containing dynamic layer of pectinase activated magnetic nanoparticles (Enz^{SP}), parallel control filtration cell containing dynamic layer of neutral magnetic nanoparticles (NP^{SP}) and two parallel permeate tanks and digital manometers.

2.2.6. Long term stability

The BMR^{SP} was continuously operated over 174 and 224 h at 40 °C and 25 °C respectively, to measure the rate of enzyme deactivation, enzyme leakage and its long term operability. For this particular test, the experimental conditions were: flux: 5 L/m² h, feed concentration: 0.3 g/L, amount of Enz^{SP} per membrane area: 3 g/m².

3. Results and discussion

3.1. Membrane characterization

The enzyme loading capacity measured by directly injecting Enz^{SP} into a Bicinchoninic acid assay (BCA) solution was 246 mg/g of NP^{SP} . The average pore size for the prepared membrane, both in the presence and absence of 4.8 mg of Enz^{SP} layer was 0.1 μm with a tortuosity factor of 0.715. Hence the presence of the Enz^{SP} layer on the membrane did not affect the membrane morphological characteristics. The dynamic layer of Enz^{SP} exhibited non-uniform aggregates with sizes ranging from 50 to 100 nm (Fig. 2-a).

Assuming the Enz^{SP} density is equal to the density of ferrous iron (5150 g/L), it has a spherical shape and absence of particle agglomeration, the porosity (ε) of the biocatalytic layer can be estimated as:

$$\varepsilon = 1 - \frac{\rho_b}{\rho_p} \quad (8)$$

where ρ_b is the bulk density (1008 g/L), calculated by weighting the mass of 1 * 10⁻³ L of NP^{SP} containing suspension.

The biocatalytic bed porosity estimated using Eq. (8) was 0.8. In another study, detailed analysis of single strips of NP^{SP} array deposited on a surface under magnetic field revealed that the width is much larger than the width of a single NP^{SP} , indicating the inevitable aggregated state of those particles [1–3]. In agreement with this, SEM micrographs in Fig. 2-a showed the presence of aggregates, resulting in the deviation from the assumptions made. Hence, ρ_p should be corrected to the density of aggregates of particles. A compact arrangement of spheres has a maximum compactness of 0.74 (i.e. a porosity of 0.26). The aggregates are not arranged on a crystalline network; hence their porosity if

probably lower and closer to the one of a cubic arrangement is 0.6. The density of one aggregate would then be:

$$\rho_a = 0.6\rho_p + 0.4\rho \quad (9)$$

Since the particle density is 5150 g/L, then the aggregate density would be ~3400 g/L and the estimated porosity of the bed of aggregates would then be around 0.7 corresponding to a highly porous biocatalytic layer. In agreement with this, the SEM cross-sectional view in Fig. 2-b revealed a highly porous 2 μm thick Enz^{SP} layer on the top of the membrane. The formation of this porous Enz^{SP} layer using particles at nanometer-scale can be attributed to the unique alignment of the Enz^{SP} individually or in cluster in response to the external magnetic field. When an external magnetic field was applied parallel to the surface of the M^{SP} , the Enz^{SP} dispersed in the bulk stream were aligned parallel to the applied magnetic field [1,4,5]. On the contrary, particles coming close to each other with the magnetization direction parallel repel each other, thus leaving spaces between the aligned nanobiocatalysts. This special arrangement and pattern thus provided the high degree of freedom to create a highly porous biocatalytic layer (with estimated bead porosity of 70% e.g., at 2 μm thick layer of Enz^{SP}).

3.2. Estimation of Peclet number (Pe)

In a continuously operated reactor, back-mixing processes can be involved. They originate in molecular diffusion of components as well as in the hydrodynamic characteristics of the solvent flow that eventually causes axial dispersion [21]. In this reactor, evaluating the presence of back-mixing of GalA is important as this may also affect the reactor performance. An empirical relation between the rates of convective transport of product in the flow direction balanced by its diffusive transport normal to the surface by the Peclet (Pe) number was used:

$$Pe = \frac{Lu_0}{D} \quad (10)$$

where D is the diffusion coefficient of GalA (5 * 10⁻¹⁰ m²/s), which was taken by comparison to the diffusivity of other molecules of similar molecular weight, u_0 is the superficial velocity (m/s) calcu-

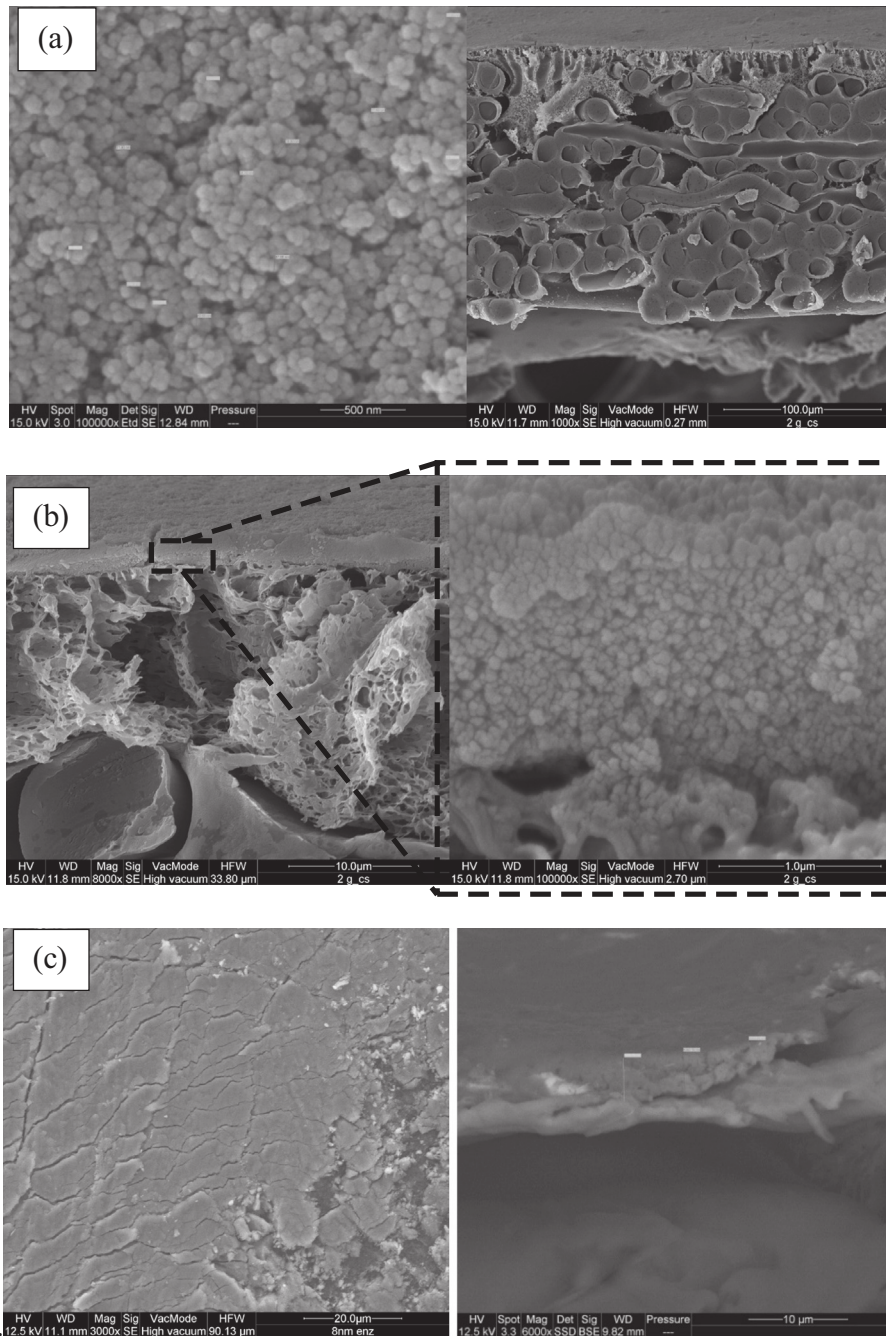


Fig. 2. a): Surface and b): cross-sectional SEM image of the biocatalytic layer containing 4.8 mg of Enz^{SP}, revealing an average bed thickness of 2–3 μm on the top of the membrane active layer. c): Surface and cross-sectional SEM image of fouled membrane with a total thickness of foulant plus nanoparticle corresponding to 4 μm after continuous filtration of 0.3 g/L pectin for 6 h on a dynamic layer containing 4.8 mg of Enz^{SP}.

lated from the permeate flux and L' is the effective diffusion length (m). Since the filtration cell is unstirred, L' is defined as the height of the filtration cell (0.06 m). The Pe numbers at different flowrates corresponding to different transmembrane fluxes are depicted in Table 1. They are larger than 1 in the whole flux range, implying that convective transport exceeds back-diffusion. Hence, back diffusion of GalA into the retentate is not expected to be significant in our conditions. More pragmatically, since the rate of convection is faster than back-diffusion, the entire GalA should be found in permeate. Therefore, measuring the GalA in permeate alone can allow us to calculate a reliable degree of conversion or rate of reaction.

Table 1

Relation between flux and ratio of convective and diffusive transport of GalA. Diffusion coefficient of GalA taken as $5 \cdot 10^{-10} \text{ m}^2/\text{s}$.

$J \text{ (L/m}^2 \text{ h)}$	$u \text{ (}\times 10^{-6} \text{ m/s)}$	Pe
5	1.38	167
15	4.16	500
30	8.33	1000
45	12.5	1500

3.3. Effect of Feed flowrate (flux)

Since the filtration was carried out under constant flux, the stability of the reactor was characterized by the rate of TMP change over time, named here as “rate of fouling” and defined as:

$$\text{Rate of fouling} = \frac{d\Delta P}{dt} \quad (11)$$

The rate of fouling was estimated from a linear curve fitting on the TMP versus time plot. Since the TMP versus time curve was accompanied by a fast rise in the first 20 min and a less intense increase from 20 to 360 min, two regions were identified for the rate of fouling. The rate of fouling in region two is indicative of a cake formation on top of the dynamic layer whereas fouling in region one reflects the initial mechanisms that partially block the membrane surface or both the membrane and the biocatalytic bed.

The TMP trend of a BMR^{SP} and a parallel control system at 5 and 45 L/m² h is shown in Fig. 3-a. This figure is an illustration of the role of the enzymatic degradation on the rate of fouling. Two different, extreme, situations can be observed here: at low flux and in the presence of Enz^{SP} at the surface, the TMP was soon stabilized, whereas this was not the case at high (45 L/m² h) flux.

Fig. 3-b shows the effect of flux on the rate of fouling (Eq. (11)) for a BMR^{SP} and a parallel control system. The rate of fouling was highly dependent on the transmembrane flux. For both systems, the rate of fouling shows an initial stage lag phase followed by a fast rise at higher flux. The ratios of rate of fouling of the control

reactor to the BMR^{SP} in region one were 1.3, 1.26 and 2 at 5, 15 and 45 L/m² h respectively while in region two they were 20, 10 and 3 respectively. Hence in region one both systems experienced similar extent of rate of fouling while the biocatalytic effect of the Enz^{SP} created a visible performance difference in region two. This ratio was significantly higher at lower flux range than at higher flux range. This could be explained because the reaction rate and the convection are of comparable magnitude at lower fluxes, thus allowing most of the pectin transported to the membrane surface to be turned into GalA, which does not accumulate on the membrane or in the retentate solution. At high fluxes, the reaction rate is small or negligible compared to the convection, leading to an accumulation of non-reacted pectin on the membrane (see Fig. 2-c).

An optimum operating condition for the BMR^{SP} would allow its operation at zero “rate of fouling” or at least at a value agreed as sustainable, considering the expected duration of a process. If one can determine the level of rate of fouling that is acceptable in a process, then the maximum constant flux (here named as J_s for “sustainable flux”) that can be applied can easily be obtained from the rate of fouling curve of the BMR^{SP}. As for example in Fig. 3 a flux of 35 L/m² h (Fig. 3-b) could be chosen for a feed containing 0.3 g/L pectin at 3 g/m² Enz^{SP} if a rate of fouling of 0.2 bar/h is considered as acceptable.

The degree of conversion measured by assaying GalA in the BMR^{SP} permeate stream at each flux value was constant over time (Fig. 3-c) i.e. no loss of enzyme activity or enzyme leakage was

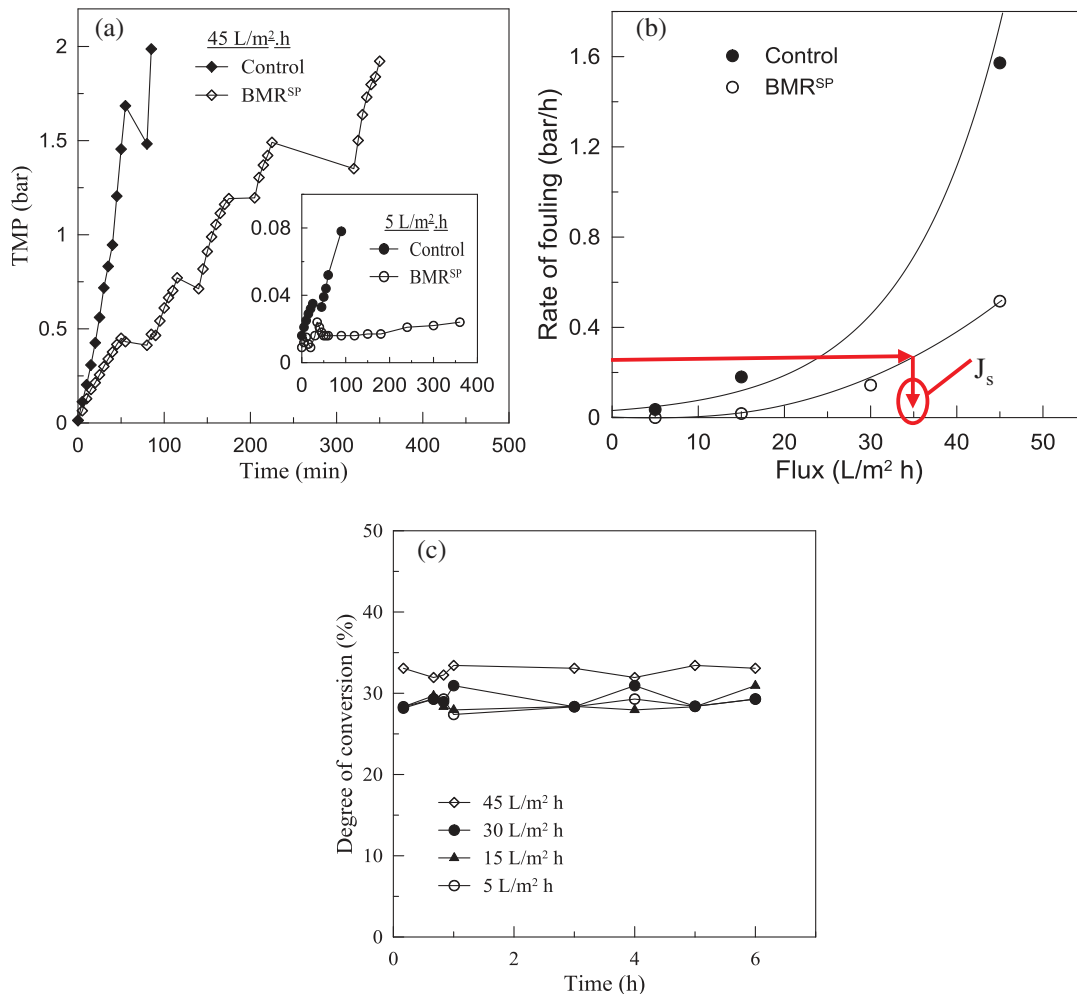


Fig. 3. a) The TMP profile of BMR^{SP} and a parallel control system at 5 and 45 L/m² h, b) relation between flux and c) degree of conversion at each flux values, at 0.3 g/L feed concentration, 40 °C and pH 4.5 (results are within 5.2% experimental error).

observed. The average degrees of conversion at 5, 15, 30 and 45 L/m² h were found to be 28, 31, 28 and 34 ± 5.2% respectively (Fig. 3-b). The degree of conversion is generally influenced by the residence time until all the enzymes get saturated by substrate. In the present case, as a result of high mass transfer rate that saturated the enzyme shortly after the onset of filtration, similar degrees of conversion for all flux values were obtained.

3.4. Effect of temperature

The thermal stability of the BMR^{SP} was studied at 25 °C and 40 °C as shown in Fig. 4. 40 °C is the optimum temperature at which the enzyme pectinase provides the best efficiency [17]. The TMP at 40 °C required to keep the flux constant at 15 L/m² h for a 0.3 g/L feed concentration reached an almost constant value at 40 °C, whereas it kept increasing over 3 h when the system temperature was set at 25° (Fig. 4). The TMP reported in Fig. 4 were corrected for the variation in feed viscosity at both temperatures. The degrees of conversion at both temperatures were constant over time (see Fig. 7-b), while the average degree of conversion revealed a 30% difference also ascribed to 40 °C being the optimal temperature in terms of pectinase activity. For this reason, the reaction rate is sufficient at 40 °C to compensate the rate of convection of pectin towards the membrane surface whereas at 25 °C, this rate of reaction being slower, an accumulation of unreacted pectin creates an additional hydraulic resistance, inducing a constant raise in the TMP.

3.5. Effect of feed concentration

The feed concentration in the reactive filtration was varied over a broad range (0.01, 0.1, 0.3, 1 and 3 g/L), at 40 °C, 15 L/m² h flux and 3 g/m² Enz^{SP} corresponding to 2 μm reactive thickness (Fig. 2-a, and L in Eq. (4)).

Fig. 5-a shows that at 3 g/L feed concentration, the TMP rises linearly. On the contrary, at low concentration (0.01 to 0.3 g/L), the TMP arrives at a quasi-steady state. This trend further implies that the BMR^{SP} can be operated under these concentrations and a reasonable flux of 15 L/m² h without a significant increase in TMP further to the initial one, which is ascribed to the fouling of the layer of nanoparticles or of the membrane surface.

Only the reaction rates in the absence of membrane fouling were taken into consideration so as to apply Eq. (1). Hence, the

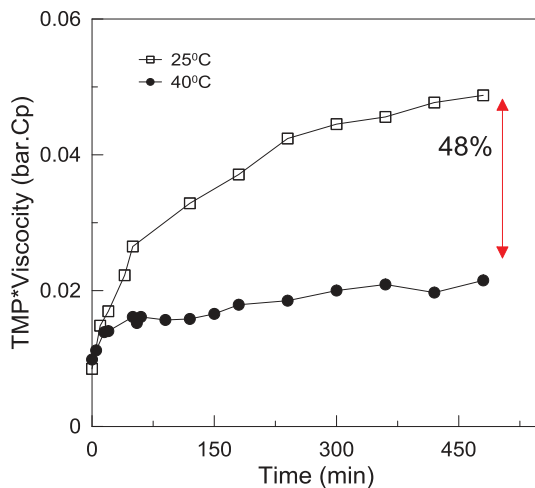


Fig. 4. Effect of temperature on the transmembrane pressure development: 0.3 g/L feed concentration, 15 L/m² h flux, the TMP in the y-axis is normalized by the viscosity of the feed solution at 25 °C and 40 °C.

kinetic parameters were calculated for the feed concentration between 0.01, 0.1 and 0.3 g/L.

The total bed volume, V_T estimate from Eq. (4) was $3.2 * 10^{-6}$ L while the actual reactor volume, V_a from Eq. (6) was $2.24 * 10^{-6}$ L. This value was further used to calculate v_r in the BMR^{SP} according to Eq. (7). The BMR^{SP}'s apparent Michaelis-Menten constant K_m^{app} and the apparent maximum reaction rate v_{max}^{app} obtained from the Lineweaver-Burk plot (Fig. 5-c) were 0.58 g/L and 31 M/h, respectively. The v_{max}^{app} obtained here was significantly higher than the v_{max} (0.07 M/h) of a free enzyme obtained in a stirred tank reactor. Nevertheless, both systems revealed equivalent K_m (0.51 g/L) values. The free enzyme reactor kinetic performance was obtained in the presence of enzyme-product inhibition with an inhibition constant of 0.31 g/L [17]. A much better biocatalytic efficiency was obtained in the BMR^{SP} attributed to an absence of enzyme-product inhibition and a high mass transfer rate induced by the convective flow through the bed of nanoparticles [22], which was operated under reaction rate limited condition. Furthermore, for a given velocity the use of a bed of nano-sized particles enhances the mass transfer phenomena thereby attributed to the reaction rate-limited conditions [23].

In Fig. 3-b, at 0.3 g/L feed concentration, the flux J_{opt} (Eq. (12)) at which an almost zero rate of fouling occurred was 5 L/m² h.

$$J_{opt} = \frac{\gamma}{C_f} \quad (12)$$

where, C_f is feed concentration (g/L) and γ is the BMR^{SP} productivity (g/m² h).

If one assumes that the flux is maintained constant because the enzymatic degradation of pectin exactly compensates its convection $J.C_f$, then the value of γ is 1.5 g/m² h. When the feed concentration was set to 0.1 g/L, J_{opt} was 15 L/m² h (Fig. 5-b). In other words, γ has the same value of 1.5 g/m² h. Accordingly, if the value of J_{opt} was fixed at 45 L/m² h, one would need to reduce the feed concentration to 0.01 g/L to attain zero rate of fouling.

A BMR^{SP} is thus characterized by a unique productivity (γ) to digest a given load of substrate (here ~1.5 g/m² h). By adjustment of the product (filtration flux by substrate concentration), one can match this productivity and obtain a steady state regime, corresponding to a nil accumulation term in Eq. (1). One can then define an optimal filtration flux for such BMR^{SP}s as the flux beyond which a continuous increase in transmembrane pressure would be observed, and below which a steady state would be observed, at least as long as the enzyme activity would remain constant. The challenge would be, by increasing the enzymatic efficiency, to increase the value of γ i.e. to increase the absolute value of the initial offset for J_s with an amendable rate of fouling in Fig. 3-b or J_{opt} for a given feed concentration in Fig. 5-b.

3.6. Effect of enzyme concentration

Fig. 6 shows the effect of the amount of enzyme immobilized per membrane area on BMR^{SP} at 15 L/m² h, 0.3 g/L feed concentration and 40 °C.

The rate of fouling showed a significant reduction when the amount of enzyme increased, despite the increase in thickness of the dynamic membrane. This is attributed to the special alignment of Enz^{SP} in response to the external magnetic field that created a highly porous biocatalytic layer (Fig. 2) and presence of particles size distribution due to the aggregate formation that tends to distribute the flow more uniformly over the cross-section.

The non-linear relation perhaps is due to the tendency of the Enz^{SP} to form aggregates at higher concentration. The formed aggregates may eventually cause partial loss of biocatalytic sites.

A larger amount of Enz^{SP} allowed an enhanced conversion of substrate. As a result, it was possible to reach a degree of conver-

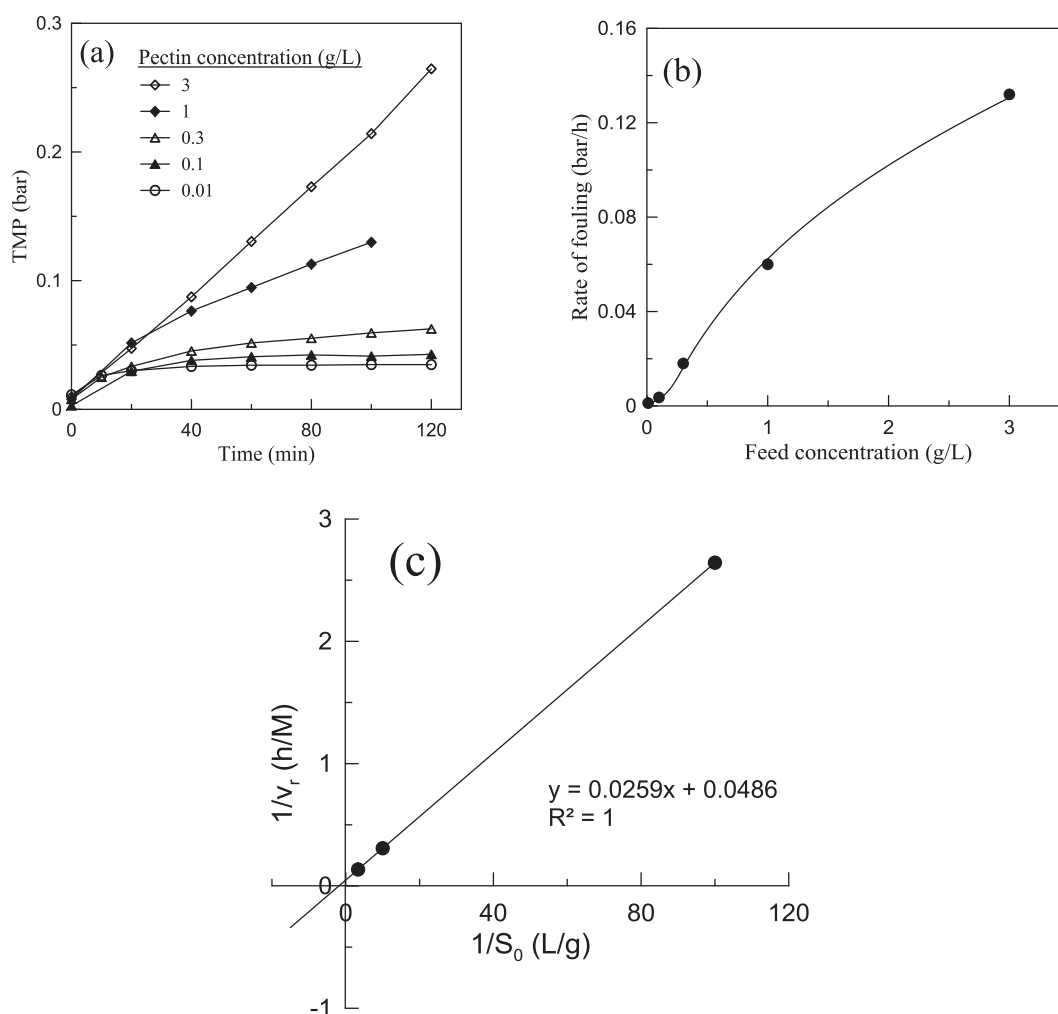


Fig. 5. Relation between a) feed concentration and TMP, and b) feed concentration, degree of conversion, rate of fouling and amount of GalA produced at $15 \text{ L/m}^2 \text{ h}$, 40°C and pH 4.5. c) Lineweaver-Burk plot.

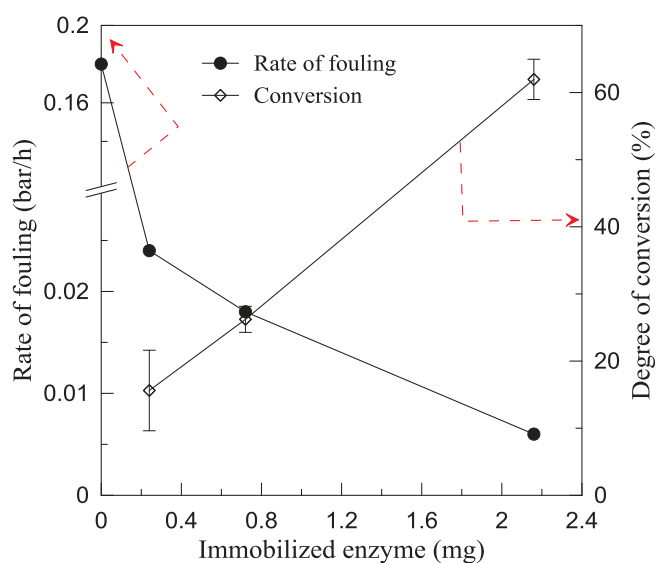


Fig. 6. Effect of amount of Enz^{SP} deposited per membrane area on the rate of fouling and degree of conversion. The transmembrane flux was fixed at $15 \text{ L/m}^2 \text{ h}$, temperature 40°C and pH 4.5.

conversion as high as 60% at $9 \text{ g/m}^2 \text{ Enz}^{\text{SP}}$. The aforementioned need for higher BMR^{SP} productivity, γ , by increasing the enzymatic efficiency was therefore attained here by increasing the amount of Enz^{SP} loading.

3.7. Long-term stability

Among the main limitations of a BMR are the losses of enzyme activity over time and enzyme leakage through membrane pores which eventually limit its long term operability. The developed system showed an interesting performance over a broad range of operational conditions. It is thus imperative to verify its time stability by conducting filtration over long periods. In our previous work, it was shown that when the system was operated over five cycles comprising an 8 h continuous filtration at $17 \text{ L/m}^2 \text{ h}$, a step-by-step decrease in performance was observed. This was attributed to the mass transfer rate exceeding the reaction rate [5]. In the present work, we then set our system in conditions where the mass transfer rate is balanced by the reaction and decided to run the reactor for a much longer period of time that would exceed a production cycle of a week in an industry. For a feed concentration of 0.3 g/L , the flux was set at $5 \text{ L/m}^2 \text{ h}$ at which a very low rate of fouling has been observed (Fig. 3-b).

Fig. 7a-b shows the variation in TMP and enzyme activity over time when the system was continuously operated at $5 \text{ L/m}^2 \text{ h}$ for

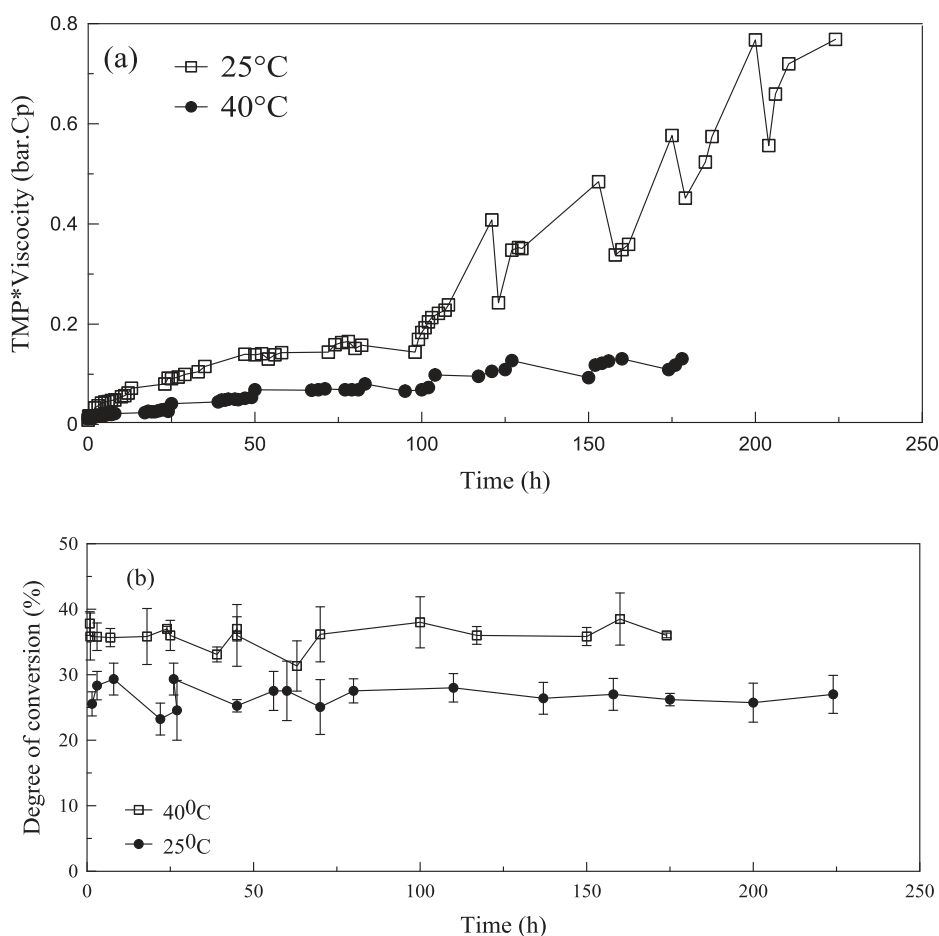


Fig. 7. Operational stability of BMR^{SP} operated at 0.3 g/L, 5 L/m² h and 3 g/m² (2 μm) Enz^{SP}, constant magnetic field, operated continuously for two weeks: a) TMP trend at 25 °C and 40 °C, b) Degree of conversion at 25 °C and 40 °C.

about two weeks at pH 4.5 both at 25 °C and 40 °C. In order to account for the viscosity change due to the temperature difference, the reported TMP was normalized by the corresponding viscosity values. Fig. 7-a shows how the TMP remained constant for 2 weeks at 40 °C. When the experiment was run at 25 °C, the TMP increased continuously as the reaction rate is lower at this temperature than at 40 °C [24]. It is worth noting that the rates of TMP rise in both cases were very slow, particularly for the first six days.

According to Fig. 7-b, the immobilized enzyme did not show any enzymatic activity decay over the entire duration since the degree of conversion was constant over time. In a mass transfer limited regime, the observed activity for a given feed concentration can remain constant even though the enzyme at the interface is losing its activity due to adverse experimental conditions. Comparison of the maximum rates of reaction obtained in batch and in BMR^{SP} suggest that the latter is operated in a reaction rate limited regime. Hence, the constant enzyme activity over the entire duration in the present case is an actual representation of stable enzyme activity [24].

By properly keeping the balance between different operating parameters, it is therefore demonstrated that the reactive filtration was conducted for a long period of time without significant pressure drop. All in all, the observed possibility of operating the system continuously for long time without significant loss in enzyme activity as well as limited rate of fouling is a great improvement over the direct covalent immobilization of enzyme which is generally practiced.

4. Conclusion

The feasibility and stability of the BMR^{SP} has been investigated over a wide range of operational parameters. This system integrates an enzymatic degradation of the substrate and a separation between substrate and product inside one single device continuously fed at constant flow rate. A much higher biocatalytic efficiency was obtained in the BMR^{SP} than in a batch reactor, ascribed to an absence of enzyme-product inhibition and a high mass transfer rate induced by the convective flow through the bed of nanoparticles which was operated under reaction rate limited condition. When the feed concentration was varied by a factor of 300 (0.01–3 g/L), the rate of fouling varied only by a factor of 8 at constant membrane flux owing to the efficient biocatalytic *in-situ* foulant degrading capacity of the magnetically formed dynamic layer of Enz^{SP}. When the flux was varied from 5 to 45 L/m² h, both productivity and rate of fouling of the BMR^{SP} increased simultaneously.

As the degree of conversion was constant at different fluxes, the enzyme was always saturated with substrate over the entire range of fluxes investigated.

When the system was operated under optimal conditions i.e., mass transfer rate balanced by reaction rate, it exhibited no significantly visible performance loss, activity decay or enzyme leakage during a 200 h lasting continuous filtration.

Moreover, the BMR^{SP} was characterized by a unique productivity or specific capacity to hydrolyze a given load of pectin (1.5 g/

m² h). The results also indicate that an increase in the reactor productivity (γ) could be achieved by increasing the enzyme loading over the surface of the membrane. This further allowed the BMR^{SP} to hydrolyze higher loads ($J.C_f$) of foulants while keeping a low if not zero increase in TMP over time at constant flux.

References

- [1] P. Jochems, Y. Satyawali, L. Diels, W. Dejonghe, Enzyme immobilization on/in polymeric membranes: status, challenges and perspectives in biocatalytic membrane reactors (BMRs), *Green Chem.* 13 (2011) 1609–1623.
- [2] L. Giorno, E. Drioli, Biocatalytic membrane reactors: applications and perspectives, *Trends Biotechnol.* 18 (2000) 339–349.
- [3] C. Torras, D. Nabarlaz, G. Vallot, D. Montané, R. Garcia-Valls, Composite polymeric membranes for process intensification: enzymatic hydrolysis of oligodextrans, *Chem. Eng. J.* 144 (2008) 259–266.
- [4] M.F. Chaplin, C. Bucke, *Immobilised Enzymes and Their Uses*, Cambridge University Press, Enzyme Technology, 1990.
- [5] A.Y. Gebreyohannes, M.R. Bilad, T. Verbiest, C.M. Courtin, E. Dornez, L. Giorno, E. Curcio, I.F.J. Vankelecom, Nanoscale tuning of enzyme localization for enhanced reactor performance in a novel magnetic-responsive biocatalytic membrane reactor, *J. Membr. Sci.* 487 (2015) 209–220.
- [6] I.T. Kim, A. Tannenbaum, R. Tannenbaum, Anisotropic conductivity of magnetic carbon nanotubes embedded in epoxy matrices, *Carbon* 49 (2011) 54–61.
- [7] M.A. Correa-Duarte, M. Grzelczak, V. Salgueiriño-Maceira, M. Giersig, L.M. Liz-Marzán, M. Farle, K. Sieradzki, R. Diaz, Alignment of carbon nanotubes under low magnetic fields through attachment of magnetic nanoparticles, *J. Phys. Chem. B* 109 (2005) 19060–19063.
- [8] R. Bouskila, R. McAloney, S. Mack, D.D. Awschalom, M.C. Goh, K.S. Burch, One-dimensional alignment of nanoparticles via magnetic sorting, *Appl. Phys. Lett.* 96 (2010) 163103.
- [9] R. Field, *Fundamentals of Fouling*, Membrane Technology, Wiley-VCH Verlag GmbH & Co. KGaA, 2010, pp. 1–23.
- [10] E. Nagy, E. Kulcsár, Mass transport through biocatalytic membrane reactor, *Desalination* 245 (2009) 422–436.
- [11] J.M. Rodríguez-Nogales, N. Ortega, M. Perez-Mateos, M.D. Busto, Operational stability and kinetic study of a membrane reactor with pectinases from *Aspergillus niger*, *J. Food Sci.* 70 (2005) E104–E108.
- [12] O. Levenspiel, *Chemical Reaction Engineering*, 3rd ed., John Wiley & Sons Inc, New York, 1999.
- [13] N. Miguel-Sancho, O. Bomati-Miguel, A.G. Roca, G. Martinez, M. Arruebo, J. Santamaría, Synthesis of magnetic nanocrystals by thermal decomposition in glycol media: effect of process variables and mechanistic study, *Ind. Eng. Chem. Res.* 51 (2012) 8348–8357.
- [14] N. Miguel-Sancho, O. Bomati-Miguel, G. Colom, J.P. Salvador, M.P. Marco, J. Santamaría, Development of stable, water-dispersible, and biofunctionalizable superparamagnetic iron oxide nanoparticles, *Chem. Mater.* 23 (2011) 2795–2802.
- [15] W. Brullot, N.K. Reddy, J. Wouters, V.K. Valev, B. Goderis, J. Vermant, T. Verbiest, Versatile ferrofluids based on polyethylene glycol coated iron oxide nanoparticles, *J. Magn. Magn. Mater.* 324 (2012) 1919–1925.
- [16] Y. Li, X. Xu, C. Deng, P. Yang, X. Zhang, Immobilization of trypsin on superparamagnetic nanoparticles for rapid and effective proteolysis, *J. Proteome Res.* 6 (2007) 3849–3855.
- [17] A.Y. Gebreyohannes, R. Mazzei, E. Curcio, T. Paoeri, E. Drioli, L. Giorno, Study on the in situ enzymatic self-cleansing of microfiltration membrane for valorization of olive mill wastewater, *Ind. Eng. Chem. Res.* 52 (2013) 10396–10405.
- [18] K.C. Gross, A rapid and sensitive spectrophotometric method for assaying polygalacturonase using 2-cyanoacetamide [Tomato, fruit softening, *HortScience* (1982).
- [19] E. Bach, E. Schollmeyer, An ultraviolet-spectrophotometric method with 2-cyanoacetamide for the determination of the enzymatic degradation of reducing polysaccharides, *Anal. Biochem.* 203 (1992) 335–339.
- [20] J.V. Diaz, G.E. Anthon, D.M. Barrett, Nonenzymatic degradation of citrus pectin and pectate during prolonged heating: effects of pH, temperature, and degree of methyl esterification, *J. Agric. Food Chem.* 55 (2007) 5131–5136.
- [21] M.F. Chaplin, C. Bucke, *Enzyme Technology*, Cambridge University Press, 1990.
- [22] M.N.H.Z. Alam, M. Pinelo, K. Samanta, G. Jonsson, A. Meyer, K.V. Gernaey, A continuous membrane microbioreactor system for development of integrated pectin modification and separation processes, *Chem. Eng. J.* 167 (2011) 418–426.
- [23] H.S. Fogler, *Elements of Chemical Reaction Engineering*, Prentice-Hall, 1986.
- [24] J.E. Bailey, D.F. Ollis, *Biochemical Engineering Fundamentals*, McGraw-Hill, New York, 1986.